ORIGINAL ARTICLE

Evaluating the Performance of the Hybrid Boundary Element- Finite Element (BE-FE) Method to Solve Electroencephalography (EEG) Forward Problem Based on the Mesh Quality: A Simulation Study

Nasireh Dayarian, Ali Khadem

[1] *Department of Biomedical Engineering, Faculty of Electrical Engineering, K. N. Toosi University of Technology, Tehran, Iran*

*Corresponding Author: Ali Khadem
Email: alikhadem@kntu.ac.ir

Received: 19 February 2022 / Accepted: 27 May 2022

Abstract

Purpose: The Boundary Element (BE) and Finite Element (FE) methods are widely used numerical techniques to solve the Electroencephalography (EEG) forward problem. However, the FE Method (FEM) has difficulty in simulating current dipoles due to singularity, and the BE method (BEM) cannot simulate inhomogeneous and anisotropic conductivity profiles. Recently, a hybrid BE-FE method has been proposed to benefit from the advantages of both BEM and FEM in solving the EEG forward problem. Generally, the type of mesh may significantly influence the results of numerical EEG forward solvers and should be carefully studied.

Materials and Methods: In this paper, the performance of the hybrid BE-FE method is compared with an approach of FEM (partial integration) using three types of meshes. The ground truth is the analytical EEG forward solutions obtained from inhomogeneous and isotropic/anisotropic four-layer spherical head models with dipoles of radial and tangential directions at four eccentricities.

Results: The minimum mean of Relative Difference Measure (RDM) obtained from Partial Integration (PI)-FEM is 0.0596 at 70% source eccentricity while by using the hybrid BE-FE method it is improved to 0.0251 at the same eccentricity. On the other hand, the maximum mean of Magnitude Ratio (MAG) obtained from PI-FEM is 0.6216 at 50% source eccentricity while it is improved to 0.9734 at the same eccentricity.

Conclusion: The results show that the hybrid BE-FE method outperforms PI-FEM in solving the EEG forward problem using three types of meshes regarding RDM and MAG error criteria.

Keywords: Electroencephalography Forward Problem; Boundary Element Method; Finite Element Method; Hybrid Boundary Element–Finite Element Method; Spherical Head Model.

DOI: https://doi.org/10.18502/fbt.v10i2.12219

1. Introduction

The Electroencephalography (EEG) forward problem calculates the electric potentials on the scalp for given electrical sources in the brain. On the other hand, the inverse problem can be computed for a given forward model to find the sources that caused the measured electric potentials at the EEG electrodes, which is a very important task (called source localization) in neuroscience. An accurate solver of forward problem is required in many applications in both medical neuro-imaging and commercial applications [1, 2] since the errors caused by an inaccurate forward solver will degrade the accuracy of the inverse solution. To solve the EEG forward problem, two advanced numerical methods, including the Finite Element Method (FEM) [3, 4] and the Boundary Element Method (BEM) [3, 5, 6], have been widely applied.

The FEM is flexible for incorporating arbitrary geometries and heterogeneous and anisotropic electrical conductivity profiles, which were shown to significantly impact the current flow through biological tissues [7-9]. However, the major problem of the FEM is the singularity introduced by the dipolar source models [3, 7, 10] that are widely accepted to model EEG signal generators [11-13]. Although several approaches have been proposed to improve the performance of the FEM in singularity cases, including the subtraction method [7, 10, 14, 15], the direct method [9, 10, 16, 17], e.g., Partial Integration (PI) [17] and Saint Venant's method [16], it is still a major challenge. Also, the FEM requires discretization of the entire region into elements using an FE mesh. To improve the accuracy of EEG forward solution by FEM, the number of mesh nodes should be increased, which leads to difficult FE mesh generation and data pre-processing [8, 18, 19].

Some studies conducted on solving the EEG forward problem have used the BEM, which reformulates the forward problem with surface integrals on the boundaries of the head compartments, meaning that the linear systems to solve are considerably smaller than FEM. The BEM has numerical stability, accuracy, and effectiveness compared with differential equation-based techniques [6, 18]. The computational efficiency of BEM can be greatly increased by using acceleration techniques such as the Fast Multipole Method (FMM) [20-22]. Unfortunately, the standard BEM formulations cannot handle inhomogeneity and anisotropicity of skull/brain conductivity profile [3, 6]. A BE-inspired method has been recently proposed, which accounts for the skull and white matter anisotropy [6, 18]. However, unlike the standard BEM, which is based on surface discretization, the BE-inspired method relies on a volumetric discretization of the whole head.

To benefit from the advantages of both FEM and BEM, a combination of the BEM and the FEM can be considered. Some combinatory methods have been proposed for electromagnetic and biomedical problems [23-27], however very few ones have been proposed for solving the EEG forward problem. A 3D coupling formulation was presented in [26] to solve the EEG forward problem. This coupling method was very time-consuming because the BEM and FEM ran iteratively until the relative residuals reached below a properly set value (6×10^{-5}). Also, a relaxation parameter at each interface was compulsory to ensure convergence. The relaxation parameters were set manually, and the inappropriate value of these parameters would make the algorithm diverge. In [28], a combination of the BEM and the FEM was proposed for solving the EEG forward problem. In this hybrid BE-FE method, the isotropic and homogeneous subregions containing the current dipoles are modeled by the BEM, and the other subregions (the inhomogeneous or anisotropic subregions or those without current dipoles) are modeled by the FEM. Also, this method solves the global system in one step without any iterations. Consequently, the hybrid BE–FE method has been shown to increase the accuracy of the EEG forward solution and consequently helps to more accurate localization of brain sources.

The hybrid BE-FE method was validated in solving the EEG forward problem of isotropic/anisotropic multi-compartment media based on the conductivity uncertainties of head layers [28, 29]. The performance of numerical methods is highly dependent on the quality and number of mesh elements. However, there has been no validation of the hybrid BE-FE method or comparison with FEM in terms of the performance and computation time for different types of meshes.

In this study, the hybrid BE-FE method and FEM are compared in solving the EEG forward problem in terms of performance and computation time for three types of meshes. The EEG forward solutions are validated using the analytic solution of a four-layer isotropic/anisotropic heterogeneous spherical head model. By using the spherical head model, an approximated model of the skull as a single-layer of homogeneous and isotropic/anisotropic profile with optimized value conductivity/ anisotropy ratio is used. However, the human skull in the realistic head model has a three-layered sandwich structure, consisting of a hard (compact) bone enclosing another layer of soft (spongy) bone which is not equally thick everywhere [30].

This paper is organized as follows. In section 2, the mathematical formulations of the EEG forward problem and its numerical solutions using PI-FEM and hybrid BE-FE method will be presented. In Section 3, the performance criteria and the computation time of simulated spherical head models will be reported. In Section 4, the results will be discussed. Finally, in Section 5, the paper will be concluded, and some future works will be proposed.

2. EEG Forward Problem

2.1. Governing Equations

Consider a Three-Dimensional (3D) region Ω with conductivity tensor σ and boundary Γ. The EEG forward problem based on the quasi-static approximation of Maxwell's equations is used to estimate the electric potentials over the scalp with homogeneous Neumann boundary conditions as follows [11]:

$$\nabla.(\sigma \nabla u) = \nabla.\boldsymbol{J_P} \quad inside \;\; \Omega$$
$$\sigma \frac{\partial u}{\partial \boldsymbol{n}} = 0 \quad on \;\; \Gamma \tag{1}$$

Where u is the electric potential distribution, $\mathbf{n}$ is the outward unit vector that is normal to the boundary Γ, and $\boldsymbol{J_P}$ denotes the primary current density of the brain source [3, 11]. It is noteworthy that, in this paper, vector quantities are denoted by bold characters.

The primary current density $\boldsymbol{J_P}$ is commonly modeled as two delta functions at the current source position $\boldsymbol{r_2}(x_2, y_2, z_2)$ and the current sink position $\boldsymbol{r_1}(x_1, y_1, z_1)$ with the current source density I, as follows [9]:

$$\nabla.\boldsymbol{J_P}\,(x) = I[\delta(\boldsymbol{r}-\boldsymbol{r_2}) - \delta(\boldsymbol{r}-\boldsymbol{r_1})] \tag{2}$$

Where delta functions represent the injection of positively charged ions into the cell body of the pyramidal cells and removal of positively charged ions from the apical dendrite of the pyramidal cells at an infinitesimally small volume.

In the hybrid BE-FE method [28], the domain Ω should be divided into two regions: an outer region Ω^{FE} containing Cerebrospinal Fluid (CSF), skull, and scalp layers and an inner region Ω^{BE} containing brain layer. The outer and inner regions are formulated by the FEM and the BEM, respectively. Figure 1 depicts the two FE and BE regions. The regions Ω^{FE} and Ω^{BE} are adjacent ($\Omega = \Omega^{FE} \cup \Omega^{BE}$). Γ^{FE} and Γ^{BE} are the boundaries of Ω^{FE} and Ω^{BE}, respectively, and Γ^{int} is the interface boundary.

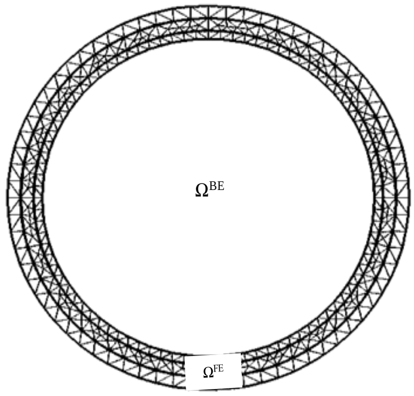

Figure 1. Domain handled by Boundary Element (BE) and Finite Element (FE) regions for the piece-wise homogenous four-layer spherical head model (brain, CSF, skull, and scalp) in the hybrid BE-FE method

2.2. FE Shape Functions

In the FE region Ω^{FE}, the domain is divided into M triangular elements and includes N^{FE} nodes. Electric potential u^e at any point within each tetrahedral element is given by linear interpolation of nodal value u_j^e [31].

$$u^e(x,y,z) = \sum_{j=1}^{4} N_j^e(x,y,z)u_j^e \tag{3}$$

Where the interpolation functions $N_j^e(x,y,z)$ are given by (Equation 4):

$$N_j^e(x,y,z) = \frac{1}{6V^e}\left(a_j^e + b_j^e x + c_j^e y + d_j^e z\right) \tag{4}$$

Where a_j^e, b_j^e, c_j^e, and d_j^e are constants and determined from the coordinates of the nodes of elements. By minimizing a functional $F(u)$ derived from the Rayleigh-Ritz method, which is a variational method, for each element and assembling all elements in the whole volume and using the PI approach to model the current dipoles [17, 32], the final set of equations can be written as follows [31]:

$$K_{FE}u_{FE} = B_{FE} \tag{5}$$

Where K_{FE} is the coefficient (stiffness) matrix, which is a function of nodal coordinates and conductivity of each element. u_{FE} is the column vector of the unknown electric potential of the nodes, and B_{FE} is the source column vector contributed by the dipoles. The electric potential is computed by applying the Neumann boundary condition, given in Equations 1, to 5.

2.3. Boundary Element Method (BEM)

In the BE region, N triangular elements at BE boundary Γ^{BE} that were produced by discretizing the FE region were used. By applying reciprocal relation to derive a boundary integral equation for the boundary value problem Equation 1 and considering constant BEs in a one-layer homogenous region, a system of N linear algebraic equations, including N unknowns is constituted as follows [33]:

$$A_{BE}X_{BE} = B_{BE} \tag{6}$$

Where X_{BE} is the column vector (column matrix), including both the electric potential u and its normal derivative $\frac{\partial u}{\partial n}$ for each element, A_{BE} is the coefficient matrix and B_{BE} is the column vector containing values of boundary condition and the current dipoles information.

2.4. Hybrid BE-FE Method

In this subsection, the EEG forward problem based on the hybrid BE-FE method is formulated. To couple BEM and FEM, the following continuity conditions must be enforced on the interface boundary Γ^{int} between the two regions Ω_{BE} and Ω_{FE} [28]

$$\varphi_{BE} = \frac{\varphi_{FE_1} + \varphi_{FE_2} + \varphi_{FE_3}}{3} \tag{7}$$

$$\sigma_{FE}\frac{\partial \varphi_{FE}}{\partial n_{FE}} = -\sigma_{BE}\frac{\partial \varphi_{BE}}{\partial n_{BE}} \tag{8}$$

where $\boldsymbol{n}_{FE}$ and $\boldsymbol{n}_{BE}$ are outward unit vectors which are normal to the Γ^{int} in the FE and BE regions, respectively. Also, φ_{BE} is the potential of BE element on interface boundary Γ and $\varphi_{FE_1}, \varphi_{FE_2}, \varphi_{FE_3}$ are the nodal potentials of the FE element corresponding to the same BE element. σ_{FE} and σ_{BE} are the conductivities of FE and BE regions, respectively. To impose Equations 7 and 8 on the interface boundary, first Equations 5 and 6 are combined and boundary conditions are applied to each interface as follows:

$$\begin{bmatrix} K_{FE} & \emptyset \\ \emptyset & A_{BE} \end{bmatrix}\begin{bmatrix} u_{FE} \\ X_{BE} \end{bmatrix} = \begin{bmatrix} B_{FE} \\ B_{BE} \end{bmatrix} \tag{9}$$

where K_{FE} and A_{BE} are the coefficient matrix of elements in FE and BE regions, respectively. B_{FE} and B_{BE} are source column vectors that existed in FE and BE regions and $\emptyset$ is the zero matrix. Also, u_{FE} and X_{BE} are the unknowns of FE and BE domains. The unknowns of the FE region are the nodal electric potential of FE elements and in the BE region are the electric potential and its normal derivative of each element.

It is noteworthy that the BEM is used to represent the Poisson Equation 1 at the brain subregion (BE region) considering the Dirichlet boundary condition and FEM is used to represent the Laplace equation $(\nabla.(\sigma\nabla\varphi) = 0)$ at other subregions (FE regions) considering Neumann condition at CSF/brain and air/scalp interfaces for the four-layer spherical head model to derive Equation 5.

Then by applying Equations 7 and 8 to 9, the matrices K_{FE}, A_{BE}, B_{FE}, and B_{BE} are modified as $\tilde{K}_{FE}$, $\tilde{A}_{BE}$, $\tilde{B}_{FE}$, and $\tilde{B}_{BE}$, respectively; and the resulting equation is obtained as:

$$\begin{bmatrix} \tilde{K}_{FE} & M_{FE} \\ M_{BE} & \tilde{A}_{BE} \end{bmatrix}\begin{bmatrix} u_{FE} \\ X_{BE} \end{bmatrix} = \begin{bmatrix} \tilde{B}_{FE} \\ \tilde{B}_{BE} \end{bmatrix} \tag{10}$$

Where M_{BE} and M_{FE} are sparse matrices constructed as a result of applying, Equations 7 and 8 to 9 respectively. Using the Gaussian elimination method, Equation 10 is solved for u_{FE} and X_{BE}.

3. Evaluation and Results

In this section, the numerical results obtained from the hybrid BE-FE method and PI-FEM are validated with an analytical solution for a four-layer isotropic /anisotropic piece-wise homogeneous spherical head model. To validate the numerical results, the Relative Difference Measure (RDM) and the Magnitude Ratio (MAG) [3, 34] have been used as follows:

$$RDM = \left|\frac{\varphi_{Ana}}{|\varphi_{Ana}|} - \frac{\varphi_{Num}}{|\varphi_{Num}|}\right| \tag{11}$$

$$MAG = \left|\frac{\varphi_{Num}}{\varphi_{Ana}}\right| \tag{12}$$

Where φ_{Ana} and φ_{Num} are analytical and numerical solutions, respectively, and | | denotes the square root of Euclidean distance. In this paper, φ_{Ana} is calculated by using the analytical solution given in [35] for spherical head models. It is noteworthy that the nearer RDM to 0 and the MAG to 1, the better EEG forward solution.

3.1. Isotropic Piece-Wise Homogenous Four-Layer Spherical Head Model

In this example, the forward problem of a four-compartment (brain, CSF, skull, and scalp) isotropic spherical head model is solved, and the hybrid BE-FE method and PI-FEM are evaluated with an analytical solution. Table 1 indicates the parameters of this model [29, 30, 36].

In order to investigate the efficiency of the hybrid BE-FE method, we use three types of meshes (Coarse Mesh (CM), Normal Mesh (NM), and Fine Mesh (FM)) to compare the performance of the hybrid BE-FE method and PI-FEM in terms of the accuracy and computational time for different degrees of freedom. The simulation results of the hybrid BE-FE method and PI-FEM are obtained on the outmost surface (scalp) of the four-layer spherical head model generated by a dipole inside the innermost layer (brain). The domain is discretized into tetrahedral volume elements for the PI-FEM by using COMSOL 5.1 and repaired by ISO2MESH [37] that provides us accurate mesh volume and surface elements.

To extract the mesh of the hybrid BE–FE method, the BE regions, and the FE regions are discretized using a surface triangular mesh and a volume tetrahedral mesh, respectively. So that the BE and FE regions in the hybrid method have the same boundary surface elements, the entire volume domain is first discretized by irregular tetrahedral volume elements, and then irregular triangular surface elements for the BE regions are extracted from the data of the tetrahedral elements. For each of the three used meshes, the number of nodes, triangular surface elements, and tetrahedral volume elements are given in Table 2.

Figure 2 and Figure 3, respectively, show the RDM and MAG of EEG forward solutions obtained by PI-FEM and hybrid BE-FE method for dipoles of radial and tangential directions located at four different eccentricities. For each model, the three types of meshes (CM, NM, and FM) were used.

Comparing the PI-FEM and hybrid BE-FE method regarding the RDM on these isotropic models (Figure 2a and Figure 3a) shows that the hybrid BE-FE method clearly outperforms the PI-FEM for dipoles of both the radial (Figure 2a) and tangential (Figure 3a) directions at all four eccentricities. For dipoles of the radial direction, the hybrid BE–FE has a maximum RDM of 0.1486 at source eccentricity of 98% for CM, and the PI-FEM has its maximum RDM of 0.1758 at the same source eccentricity and type of mesh (see Figure 2a). Also, as illustrated in Figure 2a, the hybrid BE-FE method has much smaller RDM compared with FEM in source eccentrics of 50%, 70%, and 90%. For dipoles of the tangential direction, the maximum RDM obtained from the hybrid BE-FE method is 0.0609 at the source eccentricity of 98% for CM, while the FEM has a higher

Table 1. Parameters of the concentric four-layer spherical head model [29, 36]. The conductivity values, radius, and optimized anisotropy ratio are based on [29, 36], and [30], respectively

Tissue	Brain	CSF	Skull	Scalp
Outer shell radius (cm)	7.6	8.0	8.6	9.2
Conductivity interval (S/m)	0.2200-0.6700	1.7696-1.8104	0.0016-0.0330	0.2800-0.8700
Optimized anisotropy ratio	-	-	0.0093: 0.015	-

Table 2. The number of nodes, triangular surface elements, and tetrahedral volume elements for the three types of meshes

Method	Type of mesh	Number of Nodes	Number of Triangular surface elements	Number of Tetrahedral volume elements
PI-FEM	CM	8536	------	48362
	NM	14350	------	81942
	FM	22132	------	126197
Hybrid BE-FE	CM	6673	5460	29509
	NM	10448	8520	46406
	FM	15355	12588	67576

RDM (0.076) at these eccentricities. On the other hand, the maximum RDM obtained from the PI-FEM is 0.1231 at the same type of mesh but with the source eccentricity of 50% (see Figure 3a).

Regarding the MAG (Figure 2b and Figure 3b), the hybrid BE-FE method outperforms the PI-FEM clearly. For dipoles of the radial direction, the hybrid BE–FE has a maximum MAG of 1.0976 at the source eccentricity of 90% for CM. In comparison, the PI-FEM has the worst MAG of 0.6237 at 50% for FM (Figure 2b). In the tangential direction, the worst result of MAG from the hybrid BE-FE method is 1.0408 at 98% source eccentricity for CM, while the PI-FEM has higher MAG (0.6489) at the same eccentricity and type of meshes (see Figure 3b).

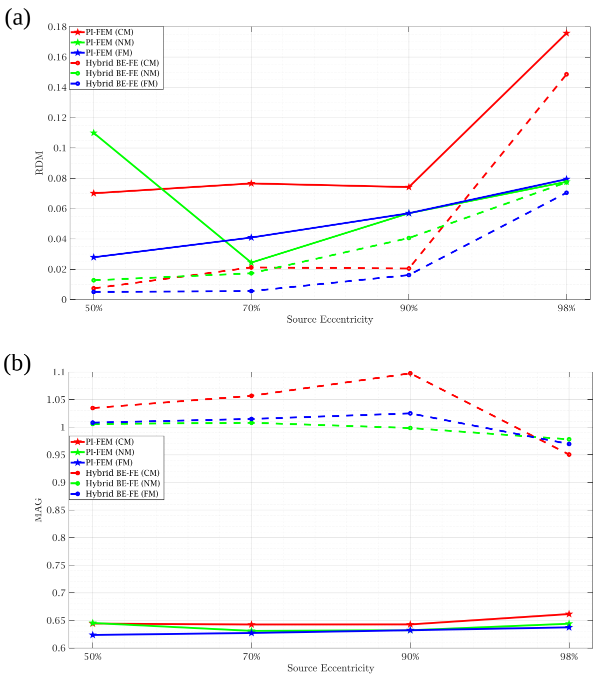

Figure 2. Isotropic piece-wise homogenous four-layer spherical head model with a dipole of radial orientation (z-axis), (a) Relative Difference Measure (RDM), and (b) MAG error of Partial Integration- Finite Element Method (PI-FEM) and hybrid BE-FE method at four different source eccentricities for three different types of meshes

3.2. Anisotropic Piece-Wise Homogenous Four-Layer Spherical Head Model

In this subsection, an anisotropic four-layer spherical head model is studied. The radius and conductivity of each layer were the same as those in Table 1, but the conductivity of the skull was anisotropic with an optimized anisotropy ratio of 0.0093: 0.015 [30]. The optimized anisotropy ratio is defined as the ratio of radial conductivity (σ_r) to tangential conductivity (σ_t) of the skull [30]. It is noteworthy that in this model, the brain (containing dipoles) is modeled by using the BEM, while other layers are modeled by using the PI-FEM.

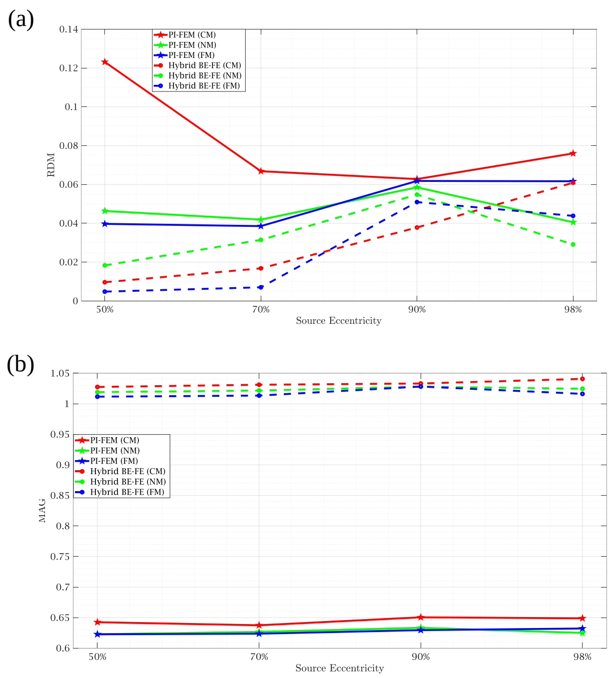

Figure 3. Isotropic piece-wise homogenous four-layer spherical head model for a dipole of tangential orientation (x-axis), (a) RDM, and (b) MAG error of PI-FEM and hybrid BE-FE method at four different source eccentricities for three different types of meshes

Figure 4 and Figure 5 show the resulting RDM and MAG for four dipole eccentricities and three types of meshes when dipoles are radial and tangential, respectively. The numbers of nodes, tetrahedral volume elements, and triangular surface elements of volume mesh are the same as the previous simulation in section 3.1.

Also, the execution times corresponding to the three cases for both the PI-FEM and the hybrid BE-FE method are compared for all eccentricities. The results showed the same profile, so one sample result for 98% source eccentricities is shown in Table 3. In this example, the Microsoft Windows 10 Enterprise N, a PC with Intel Core i7-4510U 2.6-GHz CPU and 6-GB RAM were used for both methods.

As shown in Figure 4a and Figure 5a, regarding the RDM, the hybrid BE-FE method is more accurate than PI-FEM for both dipole directions. The maximum RDM obtained from the PI-FEM in the radial direction is 0.1555 at the source eccentricity of 70% for NM, whereas, for the hybrid BE-FE method, it is 0.0274 at the same source eccentricity (Figure 4a). On the other hand, in the tangential direction (Figure 5a), the RDM obtained from the PI-FEM has a maximum of 0.133 at the source eccentricity of 50% for NM, while the hybrid BE-FE method has a maximum RDM of 0.0719 at the source eccentricity of 90%.

Also, regarding the MAG (Figure 4b) and Figure 5 b), the influence of considering the CSF layer in the spherical head model is apparent. As shown in Figure 4b and Figure 5b, the MAG error obtained from the hybrid BE-FE method is much better than PI-FEM in both directions. For radial dipoles, the best results of MAG for the PI-FEM and the hybrid BE-FE method are 0.64 at the source eccentricity of 50% for CM and 0.9056 at the same source eccentricity and type of mesh (Figure 4b). On the other hand, for tangential dipoles, the MAG obtained from the hybrid BE-FE method is better than that of PI-FEM at all eccentricities (Figure 5b).

Finally, the mean and standard deviation of RDM and MAG of all simulations were calculated at each source eccentricity. Figure 6 shows bar plots of RDM and MAG of PI-FEM and hybrid BE-FE method for isotropic and

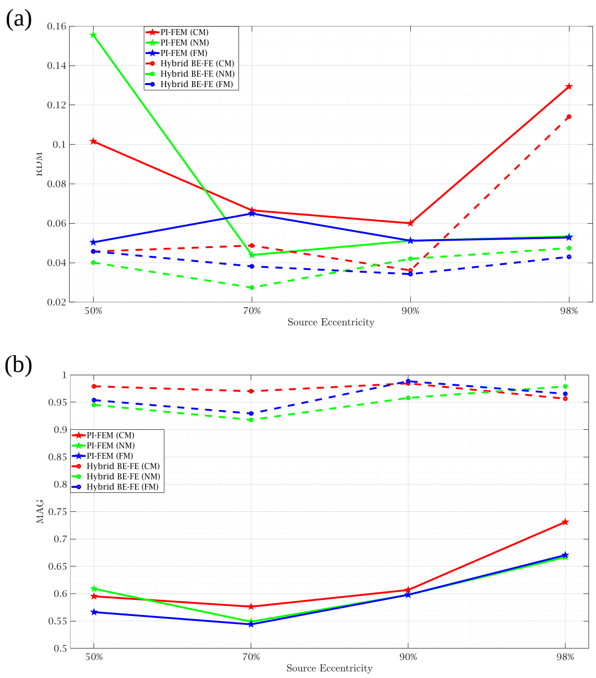

Figure 4. Anisotropic piece-wise homogenous four-layer spherical head model with a dipole of radial orientation (z-axis), (a) RDM, and (b) MAG error of PI-FEM and hybrid BE-FE method at four different source eccentricities for three different types of meshes

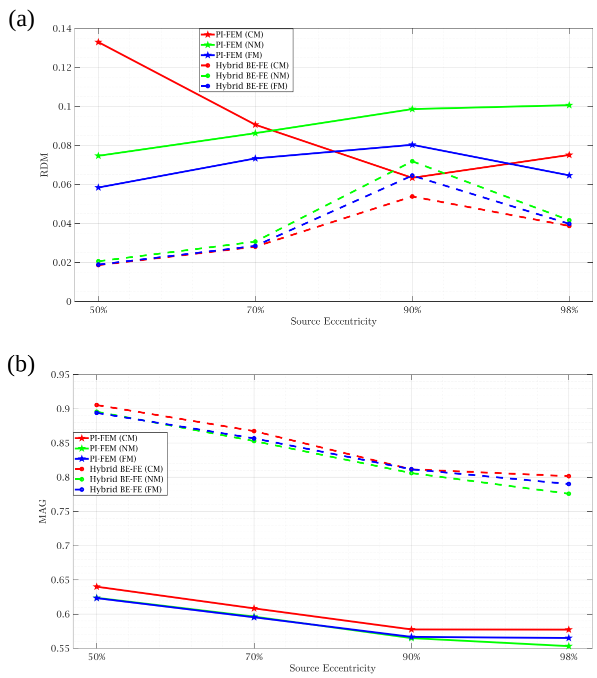

Figure 5. Anisotropic piece-wise homogenous four-layer spherical head model for a dipole of tangential orientation (x-axis), (a) RDM, and (b) MAG error of PI-FEM and hybrid BE-FE method at four different source eccentricities for three different types of meshes

anisotropic piece-wise homogeneous four-layer spherical head models versus different eccentricities for both radial and tangential dipoles. For each case, 12 realizations were simulated before. Also, the mean and standard deviation of RDM and MAG and P-values of Wilcoxon signed-rank tests are reported in Table 4. It should be noted that some results did not pass the Gaussian test (P-value < 0.05). For this reason, we used Wilcoxon signed-rank test to calculate P-values.

Comparing the PI-FEM and hybrid BE-FE method with regard to the RDM (Figure 6a and Table) shows that the hybrid BE-FE method significantly outperforms the PI-FEM for dipoles of all four eccentricities (P-value < 0.05). The hybrid BE–FE has a maximum RDM of 0.0629 ± 0.0356 at 98% source eccentricity, and the PI-FEM has RDM of 0.0778 ± 0.044 at the same source eccentricity (Figure 6a and Table). Also, the PI-FEM leads to a larger RDM variance than the hybrid BE-FE method except at 90% source eccentricity. Regarding MAG, the best result of MAG obtained from the hybrid BE-FE method is 0.9734 ± 0.0523 at 50% source eccentricity, while the PI-FEM is worse MAG (0.6216 ± 0.0229) at these eccentricities (Figure 6b and Table 4).

Table 3. Anisotropic piece-wise homogeneous four-layer spherical head model, computation time obtained for PI-FEM and hybrid BE–FE method, for three types of meshes when the current dipole is at the source eccentricity of 98%

Method	Mesh Type	Computation Time (s)
PI-FEM	CM	51.5682
	NM	151.9768
	FM	366.9810
Hybrid BE-FE	CM	76.0918
	NM	320.2645
	FM	620.4527

Furthermore, the computation time is increased from 51.5682 to 366.9810 (s) in the PI-FEM and from 76.0918 to 620.4527 (s) in the hybrid BE-FE method when CM and FM are used, revealing in all cases the execution time in the hybrid BE-FE method is more than that of in the PI-FEM (Table 3). However, using an advanced PC with a high-speed CPU and sufficient RAM, the longer execution time of the hybrid BE-FE method does not create a serious problem.

Also, regarding RDM and MAG, the hybrid BE-FE method at CM is more accurate than PI-FEM at FM except at source eccentricity of 98% in the radial direction.

4. Discussion

Although each BEM and FEM has several advantages, they also have drawbacks in solving the EEG forward problem. BEM cannot model complex geometry such as inhomogeneity and anisotropicity and head model with holes [3, 6]. On the other hand, using the FEM may cause a singularity in the right-hand side of the EEG forward Equation 1 [3, 9]. For

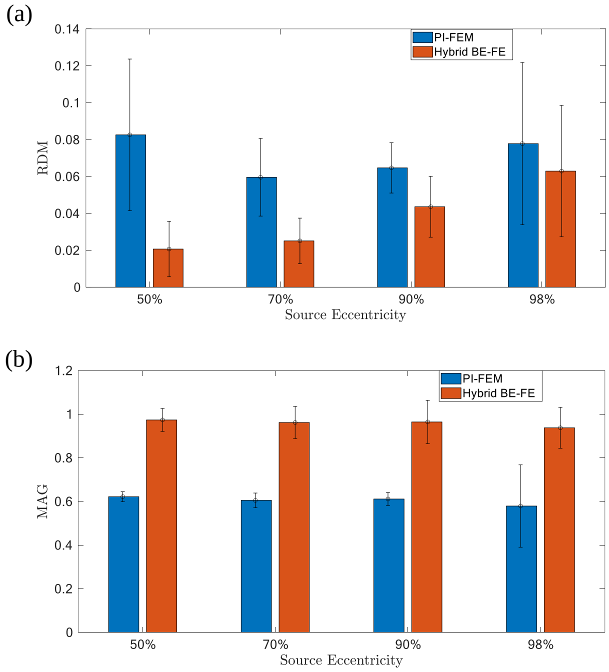

Figure 6. Mean ± std of Wilcoxon signed-rank test of 12 realizations of (a) RDM and (b) MAG of obtained from PI-FEM and hybrid BE-FE method for dipoles of four different source eccentricities

using the advantages of both methods, the hybrid BE–FE method proposed in [28] for solving the EEG forward problem offers an alternative solution. [28] compared the hybrid BE-FE method with PI-FEM for different conductivities of head layers. However, the numerical method was highly dependent on the quality of the mesh and its number of elements, [28] has not studied different types of meshes. In this study, we evaluated the performance of the hybrid BE–FE method for solving the EEG forward problem for three types of meshes with various qualities and numbers of elements at four different dipole eccentricities in radial and tangential directions and compared it with the performance of PI-FEM. The hybrid BE-FE method provides an elegant solution to the practical EEG forward

Table 4. Mean ± std and P-value of Wilcoxon signed-rank test of 12 realizations of RDM and MAG obtained from PI-FEM and hybrid BE-FE method for dipoles of four different source eccentricities at both radial and tangential directions. P-value corresponds to comparing the results of PI-FEM and hybrid BE-FE method

	Source Eccentricity	50%	70%	90%	98%
RDM	**PI-FEM**	0.0825 ± 0.0411	0.0596 ± 0.0210	0.0647 ± 0.0136	0.0778 ± 0.0440
	Hybrid BE-FE	0.0207 ± 0.0150	0.0251 ± 0.0123	0.0436 ± 0.0165	0.0629 ± 0.0356
	P-value	0.00049	0.00049	0.00049	0.0269
MAG	**PI-FEM**	0.6216 ± 0.0229	0.6048 ± 0.0335	0.6111 ± 0.0299	0.5789 ± 0.1887
	Hybrid BE-FE	0.9734 ± 0.0523	0.9617 ± 0.0738	0.9642 ± 0.0992	0.9374 ± 0.0936
	P-value	0.00049	0.00049	0.00049	0.00049

problem of modeling heterogeneity and anisotropicity in tissues whose boundaries are known without complex volume meshing of the whole 3D domain. It is noteworthy that in the hybrid BE-FE method, the volume meshing is not eliminated, but it is limited to regions without dipoles.

Regarding RDM and MAG, the results of the isotropic inhomogeneous four-layer spherical head model showed that the hybrid BE-FE method outperforms the PI-FEM in all eccentricities and both dipole directions (see Figure 2 and Figure 3). In the radial direction, the RDM of the hybrid BE-FE method is less than the RDM of PI-FEM, especially in CM (Figure 2a). It means that the hybrid BE-FE method can perform much better than PI-FEM even with small a number of mesh elements. Also, the hybrid BE-FE method with CM outperforms PI-FEM with FM except at 98% source eccentricity. On the other hand, the better performance of the hybrid BE-FE method in MAG is much more impressive (Figure 2b). These results are repeated for tangential direction as shown in Figure 3. As mentioned, the closer RDM is to zero and the closer MAG is to one, and hence the better performance the numerical method has. They indicate that using the hybrid BE–FE method with less tetrahedral volume elements yields a more accurate solution for the EEG forward problem than the PI-FEM does.

By considering the skull as a homogenous anisotropic layer in our models, the results showed that the hybrid BE-FE method outperforms the PI-FEM at all eccentricities in both dipole directions. In the radial direction, the RDM of the hybrid BE-FE method is much smaller than the PI-FEM (see Figure 4a). On the other hand, the difference between their RDM for the tangential direction is higher than that for the radial direction (see Figure 5a). Therefore, the hybrid BE-FE method clearly performs well and has a small RDM of less than 0.1141 for radial direction at the source eccentricity of 98% using CM and 0.0719 for tangential direction at the source eccentricity of 90% using NM. While the PI-FEM has a maximum RDM of 0.1555 at the source eccentricity of 70% using NM and 0.133 at the source eccentricity of 50% using CM in radial and tangential directions, respectively (Figure 4 a, Figure 5a). On the other hand, the MAG of the PI-FEM shows a large error for both dipole directions (Figure 4b and Figure 5b). On the other hand, the hybrid BE-FE method has the best results for both dipole directions.

In the next step, we calculated the mean and standard deviation of 12 realizations of RDM and MAG at four source eccentricities. Figure 6 and Table show that the hybrid BE-FE method has less mean of RDM and a higher mean of MAG compared with PI-FEM at all source eccentricities.

The generally higher accuracy of the hybrid BE-FE method was expected because of hypothetical contemplations behind the hybrid BE-FE method since it utilizes each of the BEM and FEM on the layers more qualified for them. It utilizes the BEM to demonstrate the layer containing dipoles to stay away from the singularity problem of the FEM. On the other side, it uses the FEM to model inhomogeneous and anisotropic compartments to conquer the BEM problem in simulating inhomogeneity and anisotropicity.

Finally, we compared the computation time of the PI-FEM and hybrid BE-FE method in the anisotropic model when the current dipole was at the source eccentricity of 98% (see Table 3). The results showed that PI-FEM is faster than the hybrid BE-FE method, especially when the mesh resolution is higher. This is because of using BEM and its computational integration. It seems that by using a high-performance computer, the computation time of the hybrid BE-FE method can be significantly decreased. On the other hand, using the FMM can decrease the computation time of high-resolution BEM very much [20-22] and can be used in the hybrid BE-FE method.

There are a few restrictions in our study that need to be considered. The hybrid BE-FE method is more time-consuming than the PI-FEM. Likewise, the mesh extraction of the hybrid BE-FE method is more complex than FEM. There are some academic software packages that produce volume mesh for the FEM very quickly and accurately. But to extract mesh for the hybrid BE-FE method, first, the volume mesh is generated and then the mesh to use in the hybrid BE-FE method will be extracted. Consequently, it is more time-consuming and complex than the FEM.

5. Conclusion

In this paper, the EEG forward problem has been solved by the hybrid BE-FE method. The PI-FEM and the hybrid BE–FE method have been implemented. These 3D numerical methods are validated with the analytical solution and compared with each other on the four-layer spherical head model. The results obtained from the hybrid BE–FE method on four-layer piece-wise homogenous isotropic/anisotropic spherical head models show that this method can use the advantages of both BE and FE methods, and the RDM and MAG error using the hybrid BE-FE method is less than that of the PI-FEM but at the cost of higher computational load. The directions of the future work can include further development of the proposed method to use in a five-layer spherical head model to consider the effect of anisotropicity of white matter. Moreover, we can compare our proposed hybrid BE-FE method with other types of FEM, such as subtraction and saint Venant's methods.

References

1- Zeynep Akalin Acar and Scott Makeig, "Effects of forward model errors on EEG source localization." *Brain topography*, Vol. 26 (No. 3), pp. 378-96, (2013).

2- Daniel Güllmar, Jens Haueisen, and Jürgen R Reichenbach, "Influence of anisotropic electrical conductivity in white matter tissue on the EEG/MEG forward and inverse solution. A high-resolution whole head simulation study." *NeuroImage*, Vol. 51 (No. 1), pp. 145-63, (2010).

3- JC De Munck, Carsten H Wolters, and Maureen Clerc, EEG and MEG: forward modeling. (*Handbook of neural activity measurement*). (2012), pp. 192-248.

4- Johannes Vorwerk, Christian Engwer, Sampsa Pursiainen, and Carsten H Wolters, "A mixed finite element method to solve the EEG forward problem." *IEEE transactions on medical imaging*, Vol. 36 (No. 4), pp. 930-41, (2016).

5- Matti Stenroos and J Sarvas, "Bioelectromagnetic forward problem: isolated source approach revis (it) ed." *Physics in Medicine & Biology*, Vol. 57 (No. 11), p. 3517, (2012).

6- Lyes Rahmouni, Rajendra Mitharwal, and Francesco P Andriulli, "Two volume integral equations for the inhomogeneous and anisotropic forward problem in electroencephalography." *Journal of Computational Physics*, Vol. 348pp. 732-43, (2017).

7- Leandro Beltrachini, "The analytical subtraction approach for solving the forward problem in EEG." *Journal of neural engineering*, Vol. 16 (No. 5), p. 056029, (2019).

8- Ibrahem Taha and Gregory Cook, "Brain sources estimation based on EEG and computer simulation technology (CST)." *Biomedical Signal Processing and Control*, Vol. 46pp. 145-56, (2018).

9- Hans Hallez *et al.*, "Review on solving the forward problem in EEG source analysis." *Journal of neuroengineering and rehabilitation*, Vol. 4 (No. 1), p. 46, (2007).

10- Norio Takahashi, Yujie Zhang, Zhuoxiang Ren, and David Lautru, "Finite element modeling of current dipoles using direct and subtraction methods for EEG forward problem." *COMPEL: The International Journal for Computation and Mathematics in Electrical and Electronic Engineering*, (2014).

11- Matti Hämäläinen, Riitta Hari, Risto J Ilmoniemi, Jukka Knuutila, and Olli V Lounasmaa, "Magnetoencephalography—theory, instrumentation, and applications to noninvasive studies of the working human brain." *Reviews of modern Physics*, Vol. 65 (No. 2), p. 413, (1993).

12- S Baillet, JC Mosher, and RM Leahy, "Electromagnetic brain mapping. Ieee Signal Proc Mag. 2001; 18 (6): 14–30." ed, (2001).

13- Jan C De Munck, Bob W Van Dijk, and HENK Spekreijse, "Mathematical dipoles are adequate to describe realistic generators of human brain activity." *IEEE transactions on biomedical engineering*, Vol. 35 (No. 11), pp. 960-66, (1988).

14- Kassem A Awada, David R Jackson, Jeffery T Williams, Donald R Wilton, Stephen B Baumann, and Andrew C Papanicolaou, "Computational aspects of finite element modeling in EEG source localization." *IEEE transactions on biomedical engineering*, Vol. 44 (No. 8), pp. 736-52, (1997).

15- Marion Darbas and Stephanie Lohrengel, "Review on mathematical modelling of electroencephalography (EEG)." *Jahresbericht der Deutschen Mathematiker-Vereinigung*, Vol. 121 (No. 1), pp. 3-39, (2019).

16- Helmut Buchner *et al.*, "Inverse localization of electric dipole current sources in finite element models of the human head." *Electroencephalography and clinical Neurophysiology*, Vol. 102 (No. 4), pp. 267-78, (1997).

17- Y Yan, PL Nunez, and RT Hart, "Finite-element model of the human head: scalp potentials due to dipole sources." *Medical and Biological Engineering and Computing*, Vol. 29 (No. 5), pp. 475-81, (1991).

18- Maxime Monin, Lyes Rahmouni, Adrien Merlini, and Francesco P Andriulli, "A Hybrid Volume-Surface-Wire Integral Equation for the Anisotropic Forward Problem in Electroencephalography." *IEEE Journal of Electromagnetics, RF and Microwaves in Medicine and Biology*, (2020).

19- Chany Lee and Chang-Hwan Im, "New Strategy for Finite Element Mesh Generation for Accurate Solutions of Electroencephalography Forward Problems." *Brain topography*, Vol. 32 (No. 3), pp. 354-62, (2019).

20- Sergey N Makarov, Matti Hämäläinen, Yoshio Okada, Gregory M Noetscher, Jyrki Ahveninen, and Aapo Nummenmaa, "Boundary element fast multipole method for enhanced modeling of neurophysiological recordings." *IEEE transactions on biomedical engineering,* Vol. 68 (No. 1), pp. 308-18, (2020).

21- Sergey N Makarov, Gregory M Noetscher, Tommi Raij, and Aapo Nummenmaa, "A quasi-static boundary element approach with fast multipole acceleration for high-resolution bioelectromagnetic models." *IEEE transactions on biomedical engineering,* Vol. 65 (No. 12), pp. 2675-83, (2018).

22- Sergey N Makarov, Matti Hämäläinen, Yoshio Okada, Gregory M Noetscher, Jyrki Ahveninen, and Aapo Nummenmaa, "Solving High-Resolution Forward Problems for Extra-and Intracranial Neurophysiological Recordings Using Boundary Element Fast Multipole Method." *bioRxiv,* p. 567933, (2019).

23- Chris P Bradley, Glen M Harris, and Andrew J Pullan, "The computational performance of a high-order coupled FEM/BEM procedure in electropotential problems." *IEEE transactions on biomedical engineering,* Vol. 48 (No. 11), pp. 1238-50, (2001).

24- J Sikora, SR Arridge, RH Bayford, and L Horesh, "The application of hybrid BEM/FEM methods to solve electrical impedance tomography's forward problem for the human head." in *XII ICEBI & V EIT Conference., Gdansk. ed,* (2004).

25- Subhadra Srinivasan, Hamid R Ghadyani, Brian W Pogue, and Keith D Paulsen, "A coupled finite element-boundary element method for modeling Diffusion equation in 3D multi-modality optical imaging." *Biomedical optics express,* Vol. 1 (No. 2), pp. 398-413, (2010).

26- Emmanuel Olivi, Maureen Clerc, and Théodore Papadopoulo, "Domain decomposition for coupling finite and boundary element methods in EEG." in *17th International Conference on Biomagnetism Advances in Biomagnetism–Biomag2010,* (2010): *Springer,* pp. 120-23.

27- P Ghaderi Daneshmand and R Jafari, "A 3D hybrid BE–FE solution to the forward problem of electrical impedance tomography." *Engineering Analysis with Boundary Elements,* Vol. 37 (No. 4), pp. 757-64, (2013).

28- Nasireh Dayarian and Ali Khadem, "A hybrid boundary element-finite element method to solve the EEG forward problem." *bioRxiv,* (2021).

29- Johannes Vorwerk, Ümit Aydin, Carsten H Wolters, and Christopher R Butson, "Influence of head tissue conductivity uncertainties on EEG dipole reconstruction." *Frontiers in neuroscience,* Vol. 13p. 531, (2019).

30- Moritz Dannhauer, Benjamin Lanfer, Carsten H Wolters, and Thomas R Knösche, "Modeling of the human skull in EEG source analysis." *Human brain mapping,* Vol. 32 (No. 9), pp. 1383-99, (2011).

31- S Gedney, "The finite element method in electromagnetics [Book Review]." *IEEE Antennas and Propagation Magazine,* Vol. 36 (No. 3), pp. 75-76, (1994).

32- Paul H Schimpf, Ceon Ramon, and Jens Haueisen, "Dipole models for the EEG and MEG." *IEEE transactions on biomedical engineering,* Vol. 49 (No. 5), pp. 409-18, (2002).

33- Whye-Teong Ang, A beginner's course in boundary element methods. *Universal-Publishers,* (2007).

34- Jan WH Meijs, Onno W Weier, Maria J Peters, and ADRIAAN Van Oosterom, "On the numerical accuracy of the boundary element method (EEG application)." *IEEE transactions on biomedical engineering,* Vol. 36 (No. 10), pp. 1038-49, (1989).

35- A Zhi Zhang, "fast method to compute surface potentials generated by dipoles within multilayer anisotropic spheres Phys." *Med. Biol,* (1995).

36- Sven Wagner *et al.*, "Using reciprocity for relating the simulation of transcranial current stimulation to the EEG forward problem." *NeuroImage,* Vol. 140pp. 163-73, (2016).

37- Qianqian Fang and David A Boas, "Tetrahedral mesh generation from volumetric binary and grayscale images." in *IEEE International Symposium on Biomedical Imaging: From Nano to Macro,* (2009): *Ieee,* pp. 1142-45.